

Oblique quasi-lossless excitation of a thin silicon slab waveguide: A guided-wave-variant of an anti-reflection coating

Manfred Hammer*, Lena Ebers, Jens Förstner

Theoretical Electrical Engineering, Paderborn University, Paderborn, Germany

Abstract: Radiation losses at a junction of high-contrast Si/SiO₂-slabs of different thicknesses can be avoided, if, for excitation by semi-guided waves, the angle of incidence is raised beyond a critical angle. By introducing an additional short waveguide segment of intermediate thickness at the junction, reflections can be suppressed; our simulations predict near-full transmittance for the thus “coated” interface. These are nonresonant effects; the structures perform adequately for incidence of semi-guided Gaussian beams of moderate widths, and for a comparatively broad wavelength range.

Keywords: photonics, integrated optics, slab waveguide junction, oblique excitation, reflection- and loss-suppression.

1 Introduction

Taper structures, and the modelling and design of these, for manifold purposes, have a decades-long history [1] in the field of integrated / waveguide optics. In the simplest case, this concerns interfaces between slab waveguides with different core thicknesses. The more recent past has seen a shift of emphasis to CMOS-compatible silicon photonics [2], with e.g. tapered connections of photonic crystals [3] or of photonic wires [4]. It is in this context of structures with high refractive index contrast that we reconsider the problem of a slab waveguide junction. The standard 2-D setting concerns a configuration, where both the structure under investigation and the solutions for the optical electromagnetic fields are constant along one of the coordinate axes. Abrupt interfaces between waveguide cores of different thicknesses typically generate pronounced reflections and scattering losses, motivating the search for efficient and preferably short taper structures.

We shall see in this paper that things change drastically, if we step to a 2.5-D framework [5, 6] with *oblique* incidence of the semi-guided waves at the junction, as illustrated in Figure 1(a). One retains a configuration where the structure is constant along one axis, but where optical fields are considered that vary harmonically along that axis, according to the given angle on incidence. As explained in Section 2, scattering into specific outgoing modes, including nonguided, radiated fields, is being suppressed for excitation at angles above certain critical levels [7, 8]. The effect relies solely on the properties of the outgoing slabs. Hence, the region around the junction can be shaped to adjust the scattering coefficients for the remaining outgoing propagating waves. Indeed, reflections can be largely eliminated, if one introduces an additional short slab segment of suitable intermediate properties at the junction. This is discussed in Section 3. In the last Section 4 we consider laterally confined Gaussian wave bundles (as opposed to the former plane waves) as an experimentally more realistic scenario of wave incidence.

Our proposal represents one example in a series of studies where the properties of “oblique semi-guided waves”, in particular the suppression of radiative losses, are being harnessed for the design of 2.5-D integrated optical structures, for various purposes, and with partly surprising properties [5, 7, 9–12]. A preliminary glimpse of the present results has been included in Refs. [8, 13]; recently, these findings led to a patent [14].

In the first place, this concerns solutions of the frequency-domain Maxwell equations in three spatial dimensions, but ones where the transmission characteristics are fully determined by a system of partial differential equations on the two-dimensional cross sectional domain. In line with our previous studies we call this “2.5-D”, to distinguish things from standard 2-D models on the one hand, and from more general “full 3-D” tasks on the other hand. (The term “2.5-D” has been used also for systems such as photonic crystal slabs [15] with predominant light propagation in a plane. This is *not* what is meant here.)

In our 2.5-D context, the familiar, here “rotated”, TE- and TM-polarized guided modes of dielectric multilayer slab waveguides remain valid local solutions for parts of the structure. While their shape in the out-of-plane

* Paderborn University, FG Theoretical Electrical Engineering Warburger Straße 100, 33098 Paderborn, Germany
Phone: ++49(0)5251/60-3560 Fax: ++49(0)5251/60-3524 E-mail: manfred.hammer@uni-paderborn.de

direction is determined by the (vectorial) 1-D mode profile, in-plane these waves show the functional behaviour of ordinary 2-D plane waves, i.e. the fields are constant (extend infinitely) in the direction perpendicular to their individual direction of propagation. In this context, we thus deal with non-leaky modal solutions that are confined along the out-of-plane axis, but are not confined along the lateral in-plane axis. This motivates the notion of “semi-guided waves”, as introduced in [5, 6], to distinguish the fields from e.g. the guided modes of channel waveguides with two-dimensional cross section, or from the wave bundles with confinement along two cross-sectional axes as considered in Section 4.

It appears that, in the field of integrated optics, the notion of an “antireflection coating” is traditionally associated with problems of coupling light into and out of circuits, i.e. with improving the transmission properties of potentially angled waveguide facets [16–18], also for elements that emit [19] or detect light [20]; a study [21] of antireflection segments in a plasmonics context is an exception. Early (and certain modern) concepts for devices in integrated optics [22], e.g. for lenses [23, 24], mirrors [22], prisms [25], or entire spectrometers [26], recognize well the frequently disregarded lateral dimension of the modes of 2-D slab waveguides [27]. These concepts however, are based mainly on moderate or low refractive index contrast, and/or on graded or indiffused refractive index profiles, where “coating” of interfaces is less likely to be relevant. If present, it is frequently called “tapering”.

2 Oblique incidence of semi-guided waves at a slab waveguide interface

We consider a junction between two slab waveguides as introduced in Figure 1. Vertically (x) guided, and laterally (y, z) non-guided plane waves come in at the junction with an angle of incidence θ . The parameters given in the figure caption (cf. also Table 2) resemble typical values for single mode Si/SiO₂-waveguides, of standard thickness [4] for the thicker feeding waveguide, and of substantially reduced core thickness for the output slab, both with an SiO₂-cover.

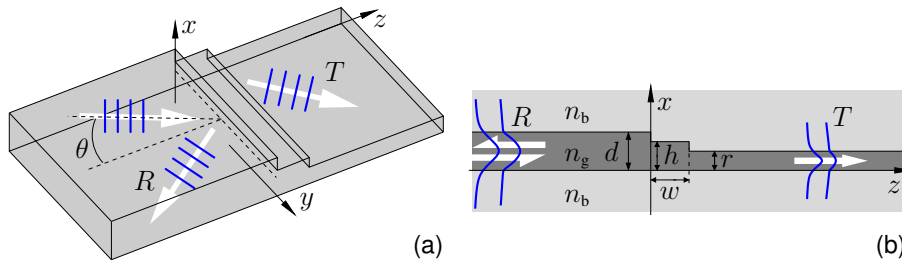


Figure 1: Artists impression (a) and cross section view (b) of the waveguide junction. Abrupt interfaces ($w = 0$) are considered, as well as “coated” structures including an intermediate segment of width w and height h , separating slabs of thicknesses $d = 0.22 \mu\text{m}$ and $r = 0.05 \mu\text{m}$ with refractive indices $n_g = 3.45$ (guiding cores) and $n_b = 1.45$ (background, substrate and cover), at a vacuum wavelength $\lambda = 1.55 \mu\text{m}$. Transmittances T and reflectances R relate to semi-guided TE-polarized excitation at angle θ .

While a more formal, general description of the vectorial effective-2-D (“2.5-D”) frequency domain scattering problem can be found in Refs. [7, 8], for the present discussion we rely primarily on simulations on the basis of a semi-analytical solver, using simultaneous eigenmode expansions along the two cross sectional coordinate axes x, z (vectorial quadridirectional eigenmode propagation, vQUEP) [6, 28]. We consider the abrupt interface ($w = 0$) first. Figure 2(a) shows angular scans of the guided-wave reflectances and transmittances.

Normal incidence at angle $\theta = 0$ relates to the standard 2-D setting with separate scalar problems for TE- and TM waves. For TE excitation one thus finds zero levels for reflected and transmitted TM polarized waves, with about 15% of the input power lost to radiated fields. Figure 3(a) illustrates the respective field on the cross section plane.

Polarizations become coupled for $\theta \neq 0$. Still, for growing θ , the scattered waves remain almost exclusively TE polarized at first, with gradually increasing transmittance, increasing reflectance, and decreasing losses. These losses vanish entirely for $\theta > 30.9^\circ$. One observes a range of angles with large TE transmittance, and noticeable reflectance for TM polarized waves. At $\theta = 37.7^\circ$, this turns abruptly to full reflection, with a major TE part, and still large, but decreasing TM reflectance. For angles $\theta > 46.3^\circ$ the TE excitation is totally reflected into semi-guided TE waves.

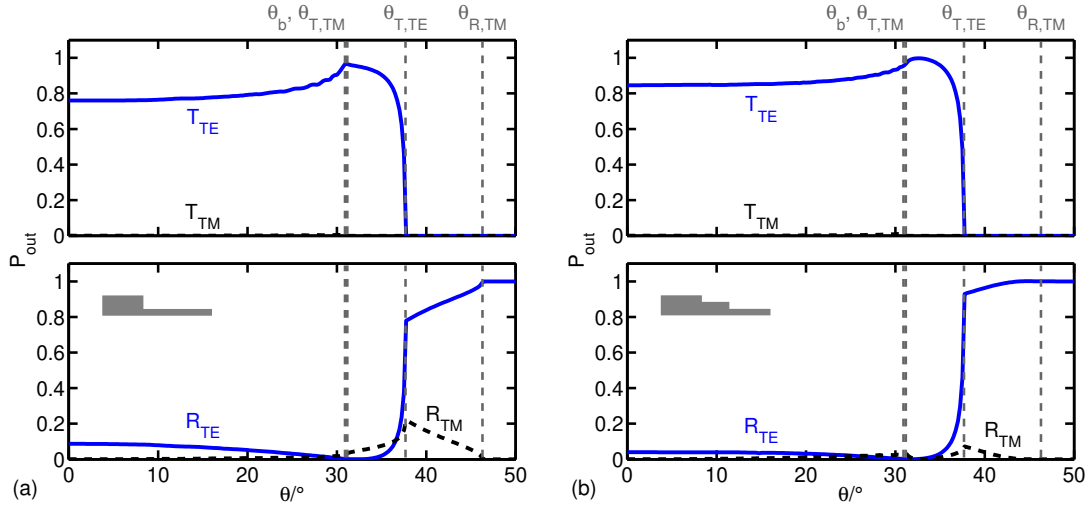


Figure 2: Transmittance T (top) and reflectance R (bottom), for scattered fundamental guided modes of TE- and TM-polarization, versus the angle of incidence θ . Critical angles θ_b for radiative losses, and $\theta_{T, TM}$, $\theta_{T, TE}$, $\theta_{R, TM}$ for the transmission and reflection into guided TE/TM waves are designated, as introduced in the text. Panels (a) relate to the abrupt interface ($w = 0$), while panels (b) show the transmission properties of the junction with an intermediate coating segment of width $w = 0.4 \mu\text{m}$, and thickness $h = 0.16 \mu\text{m}$.

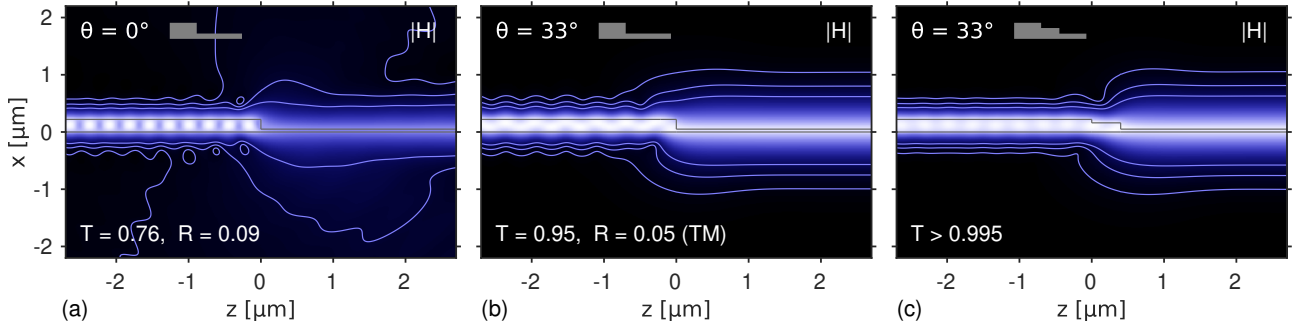


Figure 3: Propagation of semi-guided waves across the abrupt (a, b) and “coated” interface (c), for normal incidence (a), and for oblique excitation at angle $\theta = 33^\circ$ (b, c). The plots show the absolute value $|\mathbf{H}|$ of the optical magnetic field on the cross-sectional x - z -plane, with contours at levels of 2%, 5%, and 10% of the absolute field maximum (separately for each panel). Transmittance and reflectance levels T , R are shown.

Roughly, these features can be explained as follows. Slab mode analysis [29] of the two regions that support the incoming and reflected waves (thickness d) and the transmitted waves (thickness r) shows that both slabs support a fundamental guided TE- and TM-mode each, with effective mode indices $N_{R, TE} = 2.823$, $N_{R, TM} = 2.040$, $N_{T, TE} = 1.725$, and $N_{T, TM} = 1.461$. These satisfy the relations $N_{in} := N_{R, TE} > N_{R, TM} > N_{T, TE} > N_{T, TM} > n_b$, where n_b is the refractive index of the substrate and cover regions.

We are dealing with a structure that is constant along the y -axis, and that is excited by the semi-guided TE polarized wave with effective mode index N_{in} , at angle θ . Therefore the entire solution for the electromagnetic field can be restricted to the single Fourier component with wavenumber $k_y = kN_{in} \sin \theta$, for vacuum wavenumber $k = 2\pi/\lambda$, that is imprinted by the incoming wave. All outgoing waves share the respective harmonic y -dependence. Hence, each particular outgoing mode with effective mode index N_{out} leaves at an angle θ_{out} with $k_y = kN_{out} \sin \theta_{out}$ that is potentially *different* for every outgoing mode. The relation between the angle of incidence θ and the scattering angle θ_{out} can be given the form of Snell’s law:

$$N_{out} \sin \theta_{out} = N_{in} \sin \theta, \quad (1)$$

which applies to all (reflected, transmitted, up- or downwards scattered) outgoing *propagating* modes. Consequently, if, for a specific pair of modes with indices N_{in} and N_{out} , the angle of incidence is raised beyond the critical value

$$\sin \theta_{crit} = N_{out}/N_{in}, \quad (2)$$

that particular outgoing mode, and all other outgoing modes with smaller effective indices, become evanescent; these modes then do not carry any optical power away from the interface region. For our specific configuration with $N_{\text{in}} = N_{\text{R,TE}}$, this leads to the following constraints:

- All radiative, non-guided (“cladding”-) modes have effective refractive indices $N_{\text{out}} \leq n_{\text{b}}$. These become evanescent, and all radiative power loss is being suppressed, for $\theta \geq \theta_{\text{b}}$, with $\sin \theta_{\text{b}} = n_{\text{b}}/N_{\text{in}}$.
- The transmitted fundamental TM mode becomes evanescent, and the transmittance T_{TM} vanishes, for $\theta \geq \theta_{\text{T,TM}}$, with $\sin \theta_{\text{T,TM}} = N_{\text{T,TM}}/N_{\text{in}}$.
- The transmitted fundamental TE mode becomes evanescent, and the transmittance T_{TE} vanishes, for $\theta \geq \theta_{\text{T,TE}}$, with $\sin \theta_{\text{T,TE}} = N_{\text{T,TE}}/N_{\text{in}}$.
- The reflected fundamental TM mode becomes evanescent, and the reflectance R_{TM} vanishes, for $\theta \geq \theta_{\text{R,TM}}$, with $\sin \theta_{\text{R,TM}} = N_{\text{R,TM}}/N_{\text{in}}$. The input power is then fully reflected into the incident TE mode.

The respective critical angles $\theta_{\text{b}} = 30.9^\circ$ for radiation losses, $\theta_{\text{T,TM}} = 31.2^\circ$, $\theta_{\text{T,TE}} = 37.7^\circ$ for the guided TM and TE modes of the thin slab, and $\theta_{\text{R,TM}} = 46.3^\circ$ for the reflection into the guided TM mode of the input slab, are marked in Figure 2.

Our main objective is a high transmission. Hence we focus on the angles between θ_{b} and $\theta_{\text{T,TE}}$, where radiation losses are absent, while the guided TE mode can still propagate in the thin slab. The somewhat arbitrarily selected angle of $\theta = 33^\circ$ leads to a TE transmittance of 95%, which actually exceeds the level for normal incidence. The reflected power of 5% is carried mainly by the TM mode; the transmitted TE wave leaves the junction at an angle of $\theta_{\text{out}} = 63.0^\circ$. Figure 3(b) gives an impression of the corresponding field.

3 A guided-wave-variant of an anti-reflection coating

The traditional technique for suppressing reflections at an interface between dielectric media consists in introducing an additional coating layer with a specific intermediate refractive index and specific thickness [30, 31]. When translating that concept to our — now lossless — waveguide junction, a coating medium with intermediate (effective) index can be realized by an additional waveguide segment of intermediate thickness h and suitable width w , as indicated in Figure 1. By changing the thicknesses of that segment, arbitrary adjustment of the effective refractive index, for polarized waves, is possible, in principle. According to Figure 2(a), however, at an angle of incidence above 31.2° , the guided incident, reflected, and transmitted TE waves, and the reflected *TM waves* play a role in the reflection process. TE- and TM-modes, with their different effective indices, will also be relevant for the field in the coating segment. Therefore the simple standard model for the transmission through an isotropic thin film [30] cannot be applied here, as shown briefly in Appendix A. Rather, we are in a — more complicated — situation of polarized wave incidence at an interface between *anisotropic* (here effective) media [32, 33].

Hence we resort to numerical means to identify optimal parameters for the coating segment. Fortunately, the 2-D vectorial scattering problem is such that a scan over some plausible region of the h - w plane can be carried out with acceptable computational effort. Figure 4 summarizes the results. Note that, in some respects, the semianalytical eigenmode propagation scheme of our solver [6] represents an analog of the eigenwave-matrix-algebra [32, 33] for the present case of guided wave propagation along piecewise stratified media.

One observes a couple of islands in the h - w -plane with close-to-unit TE transmittance. We pick the configuration with a thickness $h = 0.16 \mu\text{m}$ and width $w = 0.40 \mu\text{m}$ for our optimized anti-reflection segment. Here the solver predicts a transmittance $T_{\text{TE}} = 0.996$, where the deviation from unity comes already close to the accuracy limit of the solver. Figure 3(c) shows the optical field around the thus coated junction.

3.1 Numerical assessment

In order to provide some further corroboration of these findings, we have repeated the simulations for the three configurations of Figure 3 using the frequency-domain finite-element solver built into the COMSOL-Multiphysics suite [34]. Convergence with respect to mesh refinement, domain- and boundary settings (PMLs),

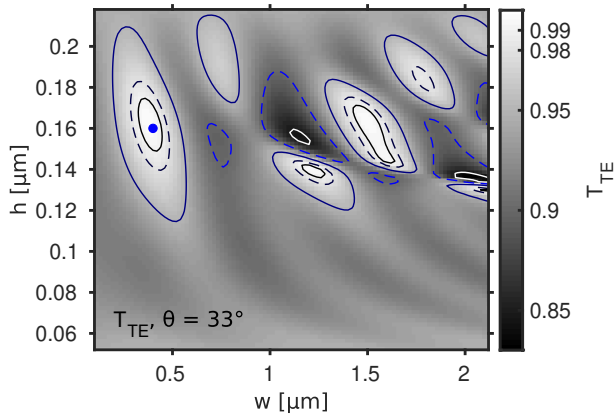


Figure 4: TE-transmittance T_{TE} as a function of thickness h and width w of the coating segment, for oblique excitation of the slab waveguide interface of Figure 1 at angle $\theta = 33^\circ$. Contours at levels of 0.85 (solid, bright), 0.9 (dashed, blue), 0.95 (solid, blue), 0.98 (dashed, black), and 0.99 (solid, black) are shown. The marker indicates the transmittance $T_{TE} = 99.6\%$ of the configuration with $h = 0.16 \mu\text{m}$, $w = 0.4 \mu\text{m}$ of Figure 3(c) and Table 2.

and solver accuracy has been assured, as far as reasonable. Table 1 shows an excellent agreement between these rigorous numerical results and the former semi-analytical vQUEP simulations.

θ	T_{TE}	R_{TE}	T_{TM}	R_{TM}	
 0°	0.760	0.087	0	0	vQUEP
	0.759	0.087	0	0	COMSOL
 33°	0.945	0.001	0	0.053	vQUEP
	0.945	0.001	0	0.054	COMSOL
 33°	0.996	0.003	0	0.001	vQUEP
	0.995	0.003	0	0.001	COMSOL

Table 1: Guided-wave transmittances T_{TE} , T_{TM} and reflectances R_{TE} , R_{TM} for the fundamental TE- and TM-polarized modes, for the three interface configurations of Figure 3. Results of simulations with the vQUEP- [6] and COMSOL-tools [34] are compared.

In case of normal incidence, $\theta = 0^\circ$, the otherwise vectorial problem separates into independent scalar problems for TE- and TM polarized waves. For pure TE excitation, all TM-related parts of the electromagnetic field are zero. At $\theta = 33^\circ > \theta_{T,TM}$, both solvers confirm that any power transfer to the TM mode of the thin slab is forbidden.

3.2 Tolerances

For an experimental realization of the coated junction concept, estimates for fabrication tolerances will be of interest. The values given in Table 2 indicate that the interface should still enable a transmittance T_{TE} higher than 99%, if a single parameter deviates from the original value q by not more than $\pm\delta q$. Modestly critical requirements are found for all parameters; the wavelength interval $\lambda \in [1.454, 1.646] \mu\text{m}$ covers the entire optical telecommunications C-band (but note that material dispersion has been neglected in the evaluation of the tolerance $\delta\lambda$ for the vacuum wavelength).

	d	r	h	w	n_b	n_g	λ	θ
q	$0.22 \mu\text{m}$	$0.05 \mu\text{m}$	$0.16 \mu\text{m}$	$0.4 \mu\text{m}$	1.45	3.45	$1.55 \mu\text{m}$	33°
δq	15 nm	5 nm	11 nm	44 nm	0.04	0.11	96 nm	0.7°

Table 2: Structural parameters q and tolerances δq for a coated interface as sketched in Figure 1. The values δq correspond to a limit $T_{TE} \geq 0.99$ for the TE-transmittance. See the text for a concise interpretation of these fabrication tolerances.

We started the design with rather arbitrarily selected parameters for the access slabs (d , r , n_g , n_b , λ), and a roughly selected angle of incidence θ ; merely the parameters h and w of the coating segment were optimized. Hence, in several cases, the actual tolerance intervals are wider than $2\delta q$, and not necessarily positioned symmetrically around the original value q . This is most notable for the thickness of the thinner slab r , and the vacuum wavelength λ .

4 Semi-guided Gaussian wave bundles

So far we have looked at incident fields that vary purely harmonically along y , i.e. that are of infinite extent in the y -direction. As a little more practically relevant approach, we now consider excitation by vertically (x) guided, laterally (y, z) wide, but localized beams. These — “true 3-D” — fields can be realized as Gaussian

superpositions of the former 2.5-D solutions, for a suitable range of values k_y around a central wavenumber $k_{y,0}$. The incoming wave bundles are thus characterized by a primary angle of incidence θ_0 , with $k_{y,0} = kN_{\text{in}} \sin \theta_0$, and further by a full width W (fields, absolute value) at 1/e-level in the y -direction, at the focus position; see Ref. [7] for explicit expressions. Figure 5 shows respective fields for incoming wave bundles of comparably (deliberately) small width $W = 10 \mu\text{m}$, focused at the origin of the y - z -plane, incident on the three junction configurations of Figure 3.

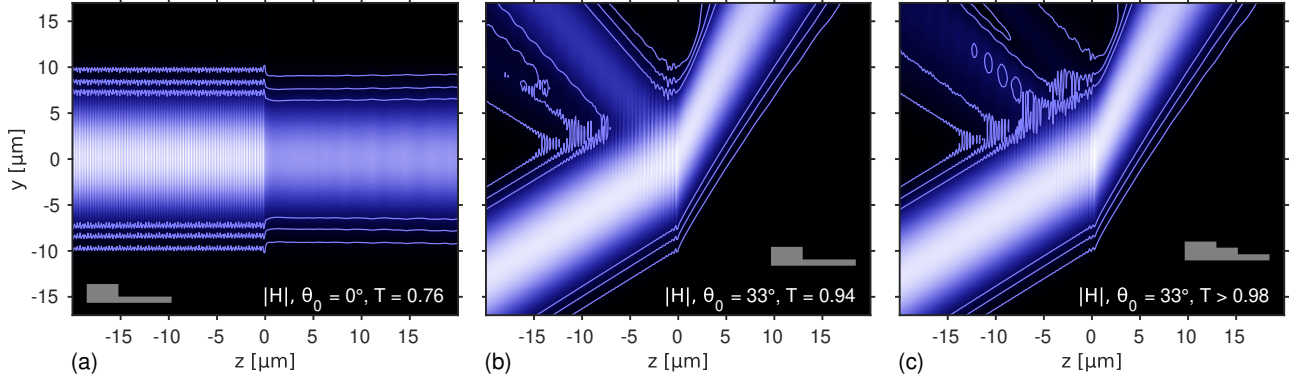


Figure 5: Semi-guided Gaussian wave bundles cross the abrupt (a, b) and coated interface (c), for normal incidence (a), and for excitation at an angle $\theta_0 = 33^\circ$. The plots show the absolute value $|\mathbf{H}|$ of the optical magnetic field, on the y - z -plane at an elevation of $x = 0.04 \mu\text{m}$ (i.e. still within the thinner core). Contours are placed at levels of 2%, 5%, and 10% of the absolute field maximum (separately for each panel). Levels of TE-transmittance T are shown.

While our coating segment has been optimized for the central angle θ_0 only, the Gaussian wave packets necessarily include 2.5-D solutions for some range of wavenumbers k_y , or for some range of incidence angles, respectively. Hence, when compared to the idealized, y -infinite configuration, the performance of the coated junction deteriorates slightly for incoming bundles of narrow widths. We expect comparable characteristics, if wave bundles of other forms are considered, such as e.g. the guided modes of wide, shallow rib waveguide [10]. For wider beams with narrower spectral width, however, the high transmittance level of the idealized structure is recovered: For incoming TE polarized wave bundles at angle $\theta_0 = 33^\circ$ of widths $W = 5, 10, 20, 40 \mu\text{m}$, the vQUEP simulations predict TE-transmittances of $T_{\text{TE}} = 0.925, 0.984, 0.993, 0.995$ for the coated junction.

5 Concluding remarks

The guided-wave scattering properties of a junction of two high-contrast silicon slab waveguides have been investigated. Oblique excitation of the interface by semi-guided waves, at a sufficiently large angle of incidence, eliminates all radiative losses. The structure can thus work as a very simple, rather short, and lossless taper; the abrupt interface generates guided wave reflections though. The configuration then resembles problems of wave incidence at an interface of anisotropic dielectric media; standard recipes for suppressing reflections through thin-film interference are not directly applicable. Still, through a rough numerical optimization procedure, we showed that near-to-unit transmittance can be realized by adding a short, suitably dimensioned waveguide segment at the junction. We have thus realized what one might call an “anti-reflection-coating” in an integrated optics setting.

Moderately critical fabrication tolerances are observed. The structure performs well also if excited by Gaussian beams of reasonable widths. This emphasizes that the scattering features of the coated junction are not, in the first place, based on resonant effects.

What concerns the adaptability of the concept, the loss suppression is clearly independent of the thickness difference, where for a lower difference than the one considered in this paper it should potentially be simpler to achieve large transmittance levels, with or even without coating segments. The critical angle relies solely on the refractive index contrast between the core (more precisely: the effective refractive index of the incident slab mode, N_{in} in Eq. (1)) and the larger one of the cladding and substrate refractive indices. These effects can be explained in terms of a negative effective permittivity [5, 8]; the arguments become relevant at moderate, i.e. not only at grazing angles, for structures with high refractive index contrast, e.g. in a context of silicon photonics.

A Comment on the effective index viewpoint

After considering Figures 1(a) and 5 one might be tempted to view our waveguide-interface-problem in a framework of effective indices. Adopting the parameters of Figure 1, and restricting things exclusively to TE-polarized waves, for the region of the original slab of thickness d we assume a homogeneous medium with (effective) refractive index $N_d = N_{R,TE} = 2.823$. Likewise, the region with reduced core thickness r is characterized by an effective index $N_r = N_{T,TE} = 1.725$. Waves travel at an angle $\theta = 33^\circ$ in the thick segment, and at an angle $\theta_r = 63.06^\circ$ in the thin output region, such that Eq. (1) holds.

Then, for full suppression of reflections, the classical recipe for an anti-reflection coating [30] demands to introduce an intermediate segment of effective refractive index $N_{h'}$, with corresponding waves at angles $\theta_{h'}$, such that the equation $N_{h'} \cos \theta_{h'} = \sqrt{N_d \cos \theta N_r \cos \theta_r}$ is satisfied, in addition to Eq. (1). For our parameters, one calculates an effective medium with index $N_{h'} = 2.053$ in which waves travel at an angle $\theta_{h'} = 48.50^\circ$. According to the solver [29] this can be realized by a waveguide of thickness $h' = 0.0859 \mu\text{m}$.

A reflectance minimum is attained [30] if the intermediate layer is of quarter-wave optical thickness $w' = \lambda/(4N_{h'} \cos \theta_{h'})$, which, for our parameters, evaluates to $w' = 0.2849 \mu\text{m}$. Indeed, a solver for optical transmission through dielectric multilayer stacks [35] predicts a transmittance $T = 1$ and reflectance $R = 0$ for the problem with refractive indices $N_d : N_{h'} : N_r$ and intermediate layer thickness w' , for s-polarized waves at angle of incidence θ and vacuum wavelength λ . One might argue that, after having considered TE-polarized waves in the first place, the “flattened” effective index setting should correspond to parallel (TM) polarization. This leads to an almost equally high transmittance $T = 98\%$ for the parameters $N_{h'}$ and w' as given.

If we return, however, to our original vectorial simulations [6] with the thus determined values h' and w' for the thickness and width of the coating segment, we get a rather meagre result of $T_{TE} = 91\%$, $R_{TE} = 4\%$, $R_{TM} = 5\%$ (cf. also Figure 4) with a transmittance that is even lower than the level for the uncoated transition (see Table 1). Apparently the effective-index viewpoint is inadequate for the present design tasks.

A similar negative result is obtained for the abrupt junction. This can be translated to a problem of angled plane wave reflection at an interface between regions with effective indices of $N_d : N_r$, for angle of incidence θ at vacuum wavelength λ . The solver [35] predicts transmittances $T = 75\%$ for s-polarization and $T > 99\%$ for p-polarized waves. The levels deviate significantly from the values $T_{TE} = 95\%$, $R_{TE} = 0\%$, $R_{TM} = 5\%$ in Table 1. Obviously, also for “pure” TE excitation, both TE- and TM-waves play a role in determining the transmittance properties of the waveguide junctions. These vector features cannot be captured with the scalar effective index models.

Acknowledgments

Financial support from the German Research Foundation (Deutsche Forschungsgemeinschaft DFG, projects HA 7314/1-1 and 231447078–TRR 142, subproject C05) is gratefully acknowledged.

References

- [1] D. Marcuse. Radiation losses of tapered dielectric slab waveguides. *The Bell System Technical Journal*, 49(2):273–290, 1970.
- [2] R. Soref. The past, present, and future of silicon photonics. *IEEE Journal of Selected Topics in Quantum Electronics*, 12(6):1678–1687, 2006.
- [3] P. Bienstman, S. Assefa, S. G. Johnson, J. D. Joannopoulos, G. S. Petrich, and L. A. Kolodziejski. Taper structures for coupling into photonic crystal slab waveguides. *Journal of the Optical Society of America B*, 20(9):1817–1821, 2003.
- [4] W. Bogaerts, D. Taillaert, B. Luyssaert, P. Dumon, J. Van Campenhout, P. Bienstman, D. Van Thourhout, R. Baets, V. Wiaux, and S. Beckx. Basic structures for photonic integrated circuits in silicon-on-insulator. *Optics Express*, 12(8):1583–1591, 2004.
- [5] F. Çivitci, M. Hammer, and H. J. W. M. Hoekstra. Semi-guided plane wave reflection by thin-film transitions for angled incidence. *Optical and Quantum Electronics*, 46(3):477–490, 2014.

- [6] M. Hammer. Oblique incidence of semi-guided waves on rectangular slab waveguide discontinuities: A vectorial QUEP solver. *Optics Communications*, 338:447–456, 2015.
- [7] M. Hammer, A. Hildebrandt, and J. Förstner. Full resonant transmission of semi-guided planar waves through slab waveguide steps at oblique incidence. *Journal of Lightwave Technology*, 34(3):997–1005, 2016.
- [8] M. Hammer, L. Ebers, A. Hildebrandt, S. Alhaddad, and J. Förstner. Oblique semi-guided waves: 2-D integrated photonics with negative effective permittivity. In *2018 IEEE 17th International Conference on Mathematical Methods in Electromagnetic Theory (MMET)*, pages 9–15, 2018.
- [9] M. Hammer, A. Hildebrandt, and J. Förstner. How planar optical waves can be made to climb dielectric steps. *Optics Letters*, 40(16):3711–3714, 2015.
- [10] L. Ebers, M. Hammer, and J. Förstner. Oblique incidence of semi-guided planar waves on slab waveguide steps: Effects of rounded edges. *Optics Express*, 26(14):18621–18632, 2018.
- [11] E. A. Bezus, D. A. Bykov, and L. L. Doskolovich. Bound states in the continuum and high-Q resonances supported by a dielectric ridge on a slab waveguide. *Photonics Research*, 6(11):1084–1093, 2018.
- [12] M. Hammer, L. Ebers, and J. Förstner. Oblique evanescent excitation of a dielectric strip: A model resonator with an open optical cavity of unlimited Q. *Optics Express*, 27(7):9313–9320, 2019.
- [13] M. Hammer, L. Ebers, and J. Förstner. Oblique quasi-lossless excitation of a thin silicon slab waveguide. XXVI International Workshop on Optical Wave & Waveguide Theory and Numerical Modeling, Bad Sassendorf, Germany, 2018, book of abstracts, 35 (2018).
- [14] M. Hammer, L. Ebers, and J. Förstner. Optischer Übergang zwischen zwei optischen Schichtwellenleitern und Verfahren zum Übertragen von Licht. German Patent DE 10 2018 108 110 B3, Deutsches Patent- und Markenamt (filed 05.04.2018, issued 31.01.2019).
- [15] C. C. Seassal, C. Monat, J. Mouette, E. Touraille, B. B. Bakir, H. T. Hattori, J. Leclercq, X. Letartre, P. Rojo-Romeo, and P. Viktorovitch. InP bonded membrane photonics components and circuits: toward 2.5 dimensional micro-nano-photonics. *IEEE Journal of Selected Topics in Quantum Electronics*, 11(2):395–407, 2005.
- [16] C. Vassallo. Theory and practical calculation of antireflection coatings on semiconductor laser diode optical amplifiers. *IEE Proceedings J – Optoelectronics*, 137(4):193–202, 1990.
- [17] M. Reed, T. M. Benson, P. C. Kendall, and P. Sewell. Antireflection-coated angled facet design. *IEE Proceedings – Optoelectronics*, 143(4):214–220, 1996.
- [18] P. Sewell, M. Reed, T. M. Benson, and P. C. Kendall. Full vector analysis of two-dimensional angled and coated optical waveguide facets. *IEEE Journal of Quantum Electronics*, 33(12):2311–2318, 1997.
- [19] T. Saitoh, T. Mukai, and O. Mikami. Theoretical analysis and fabrication of antireflection coatings on laser-diode facets. *Journal of Lightwave Technology*, 3(2):288–293, 1985.
- [20] K. M. Rosfjord, J. K. W. Yang, E. A. Dauler, A. J. Kerman, V. Anant, B. M. Voronov, G. N. Gol’tsman, and K. K. Berggren. Nanowire single-photon detector with an integrated optical cavity and anti-reflection coating. *Optics Express*, 14(2):527–534, 2006.
- [21] E.A. Bezus, D. A. Bykov, and L. L. Doskolovich. Antireflection layers in low-scattering plasmonic optics. *Photonics and Nanostructures - Fundamentals and Applications*, 14:101–105, 2015.
- [22] P. K. Tien. Integrated optics and new wave phenomena in optical waveguides. *Reviews of Modern Physics*, 49(2):361–419, 1977.
- [23] F. Zernike. Luneburg lens for optical waveguide use. *Optics Communications*, 12(4):379–381, 1974.
- [24] G. C. Righini and G. Molesini. Design of optical-waveguide homogeneous refracting lenses. *Applied Optics*, 27(20):4193–4199, 1988.
- [25] C.-C. Tseng, W.-T. Tsang, and S. Wang. A thin-film prism as a beam separator for multimode guided waves in integrated optics. *Optics Communications*, 13(3):342–346, 1975.
- [26] F. Çivitci, M. Hammer, and H. J. W. M. Hoekstra. Planar prism spectrometer based on adiabatically connected waveguiding slabs. *Optics Communications*, 365:29–37, 2016.
- [27] R. Ulrich and R. J. Martin. Geometrical optics in thin film light guides. *Applied Optics*, 10(9):2077–2085, 1971.
- [28] M. Hammer. Quadridirectional eigenmode expansion scheme for 2-D modeling of wave propagation in integrated optics. *Optics Communications*, 235(4–6):285–303, 2004.
- [29] M. Hammer. OMS — 1-D mode solver for dielectric multilayer slab waveguides. <http://www.computational-photonics.eu/oms.html>, accessed 07/2019.
- [30] M. Born and E. Wolf. *Principles of Optics, 7th. ed.* Cambridge University Press, Cambridge, UK, 1999.

- [31] H. K. Raut, V. A. Ganesh, A. S. Nair, and S. Ramakrishna. Anti-reflective coatings: A critical, in-depth review. *Energy & Environmental Sciences*, 4(10):3779–3804, 2011.
- [32] P. Yeh. Optics of anisotropic layered media: A new 4×4 matrix algebra. *Surface Science*, 96(1):41–53, 1980.
- [33] M. Schubert. Polarization-dependent optical parameters of arbitrarily anisotropic homogeneous layered systems. *Physical Review B*, 53:4265–4274, 1996.
- [34] Comsol Multiphysics GmbH, Göttingen, Germany; <http://www.comsol.com>.
- [35] M. Hammer. MULS — Oblique incidence of plane waves on dielectric multilayer stacks. <http://www.computational-photonics.eu/muls.html>, accessed 07/2019.